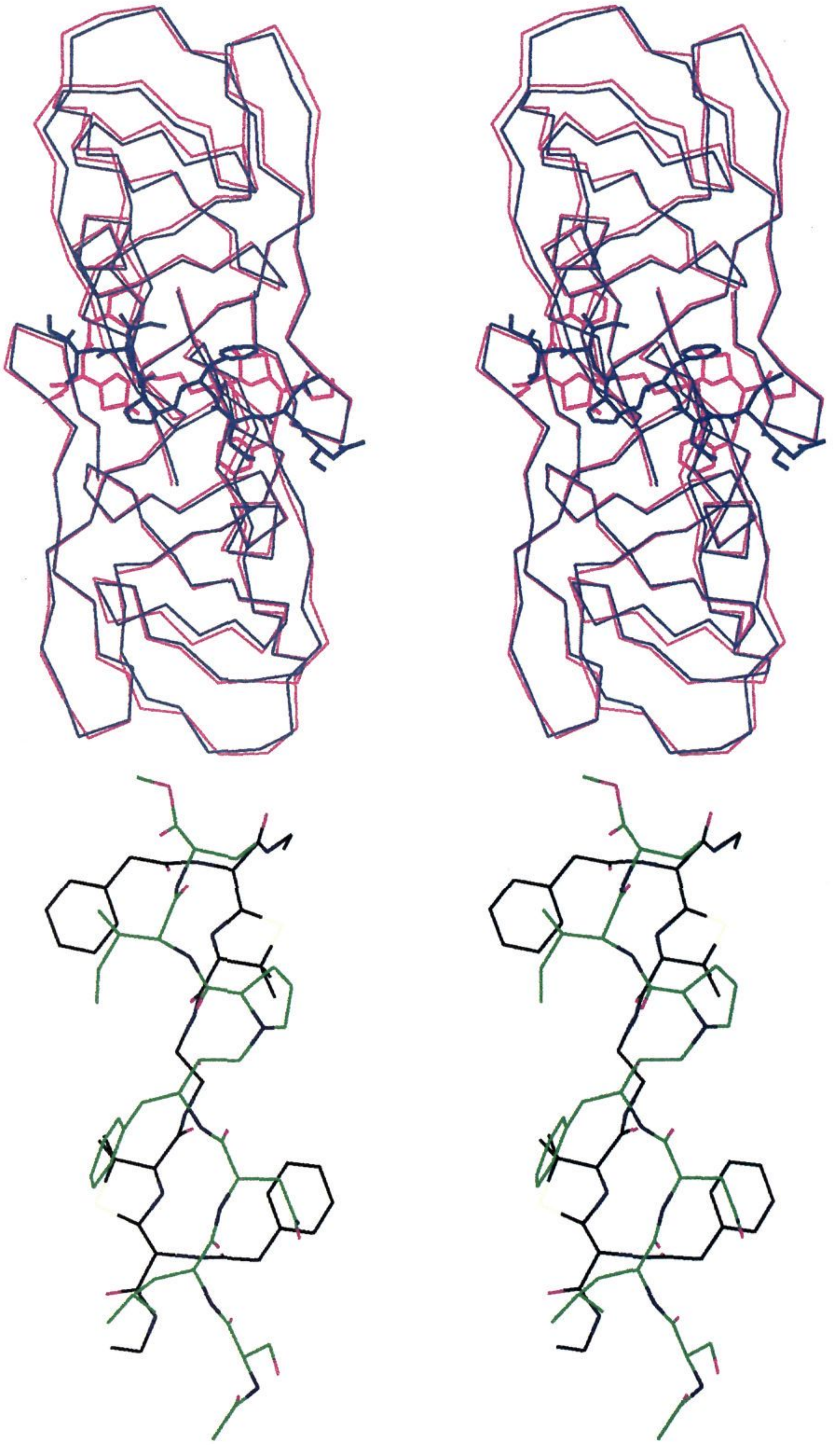

Figure 3. (a, top) Superposed Cα backbone and ligand conformations of HIVP complexes with inhibitor **1** (red) and with the peptidomimetic JG365[8] (blue). **1** traces an S-shaped course through the active site compared to the extended peptide conformation. The protein conformations are very similar. (b, bottom) Close-up of ligand overlays from complexes shown in part a.

Table II. Crystallographic Data for HIV-1 Protease Complexes

compd	space group	unit cell dimensions (Å)	resolution	R_{merge}	R_{final}
1	$P6_1$	$a = 63.4$, $b = 83.2$	2.6	0.127	0.216
2	$P6_122$	$a = 63.2$, $b = 83.3$	2.8	0.093	0.216
3	$P2_12_12$	$a = 59.4$, $b = 87.5$, $c = 46.7$	2.5	0.112	0.170

derived side chain being employed to this end.[5] The benzoyl derivative **3a** showed poor activity, and modeling suggested this was because the ring could not reach into S_2/S_2'. However the oxacillin-derived compound **3b** showed good activity against free enzyme, although it had poor whole-cell activity. Molecular modeling indicated that the phenyl substituent of the isoxazole would fit into S_2/S_2', and this observation led to the design of the orthophenyl derivative **3** in which S_2/S_2' was hypothesized to be occupied in a similar fashion. This compound was

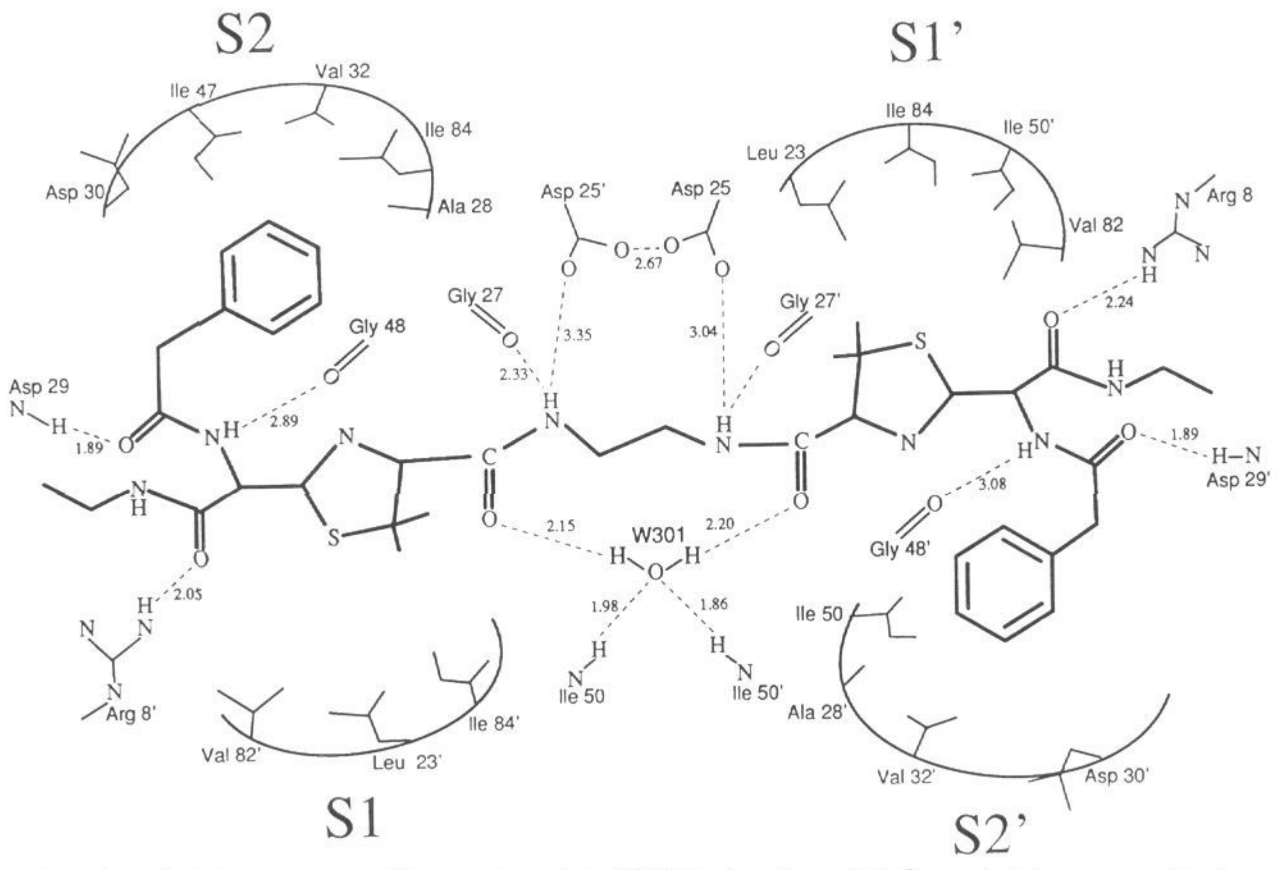

Figure 4. Diagram of nonbonded interactions of 1 complexed to HIVP taken from 2.5-Å crystal structure. Hydrogen bonds are shown as dotted lines with heavy atom distances marked (Å). It is evident that S_1 and S_2 subsites are filled with the thiazolidine and phenylacetate, respectively.

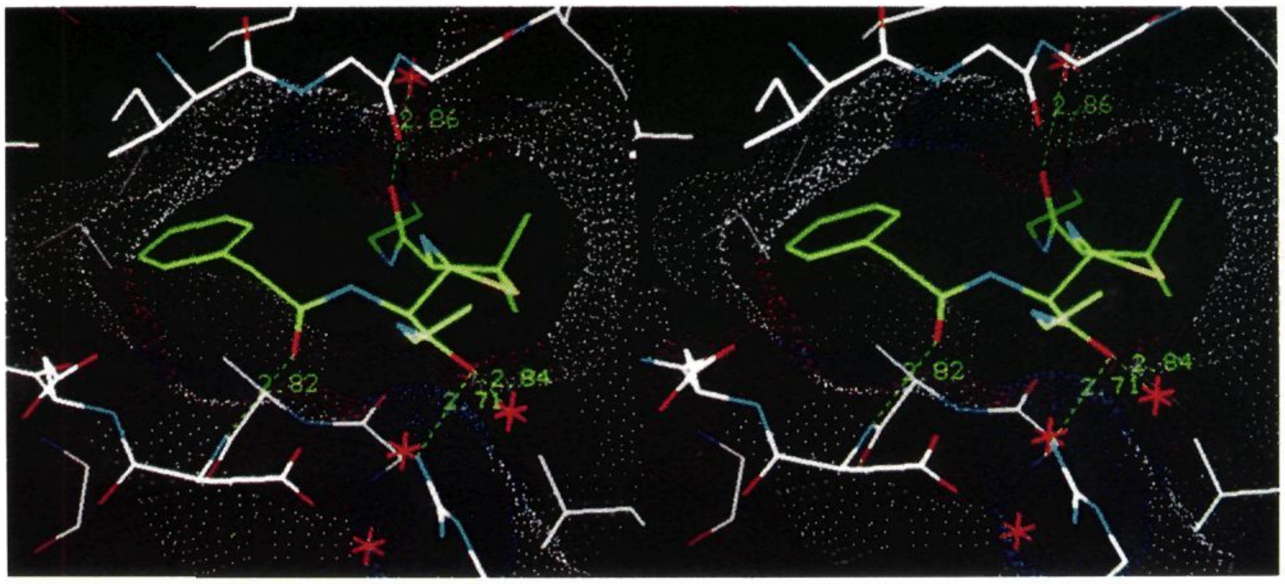

Figure 5. Connolly surface of protein S_2 and S_1 pockets showing close-packing of 1 into subsites, with the thiazolidine occupying S_1 and the penylacetate side chain in S_2.

found to be a potent inhibitor of HIVP and was also 100-fold more active than **3b** in its whole-cell activity, which may be a consequence of its increased lipophilicity. When the crystal structure of **3** was determined, the proposed mode of binding was confirmed. The additional "backbone" carbon atom of **3** causes some displacement of the substituted phenyl ring, although the contacts to the protein and space occupied are much the same as in **1** and **2**; the crucial carbonyl hydrogen bond to the NH of Asp 29 is also conserved concomitant with a change in the amide plane (Figures 4 and 6). The only significant change in the protein S_2/S_2' pocket is displacement associated with the change in torsion angle of the Asp 30/30′ side chain. Figure 7 shows the electron density of the inhibitor; the relative rotation of 60° of the *o*-phenyl ring attached to the benzoyl ring is clearly evident.

This series of penicillin-derived dimers is relatively tolerant of the β-lactam opening substituent;[5] indeed, the ammonia-opened compound has an IC_{50} of 3 nM, much more potent than some compounds with larger substituents, indicating that interactions at the edges of the active site can be deleterious.[5] Evidence for this is seen in the bound-crystal structure of compound **2**, in which the bulky phenyl ring displaces the guanidinium group of Arg 8 and therefore disrupts the conserved salt bridge between Arg 8 and Asp 29′. In compounds **1** and **3**, the smaller ethyl group packs against the Arg 8 side chain, which is moved only slightly.

Compounds **1** and **3** are C_2-symmetric and there is no evidence for asymmetry in the core region of protein or ligand in their complexes with HIVP (Figure 6). Compound **2** is pseudo-C_2-symmetric and significant asymmetry is seen in the complex, possibly due to the influence of the achiral hydroxyl (Figure 6). These results contrast with recent data on symmetric diol inhibitors[8b] which bind asymmetrically to HIVP due to dominant hydrogen bonding with Asp 25/25′.

There is no evidence for different conformations of active site side chains in different halves of the dimer in the complexes of **1**, **2**, or **3**, unlike the acetyl–pepstatin complex,[9a] possibly due to the high symmetry of the compounds. Significant differences are seen at the protein surface, due mainly to crystal packing, in the complex with **3**, which crystallizes in the orthorhombic space group

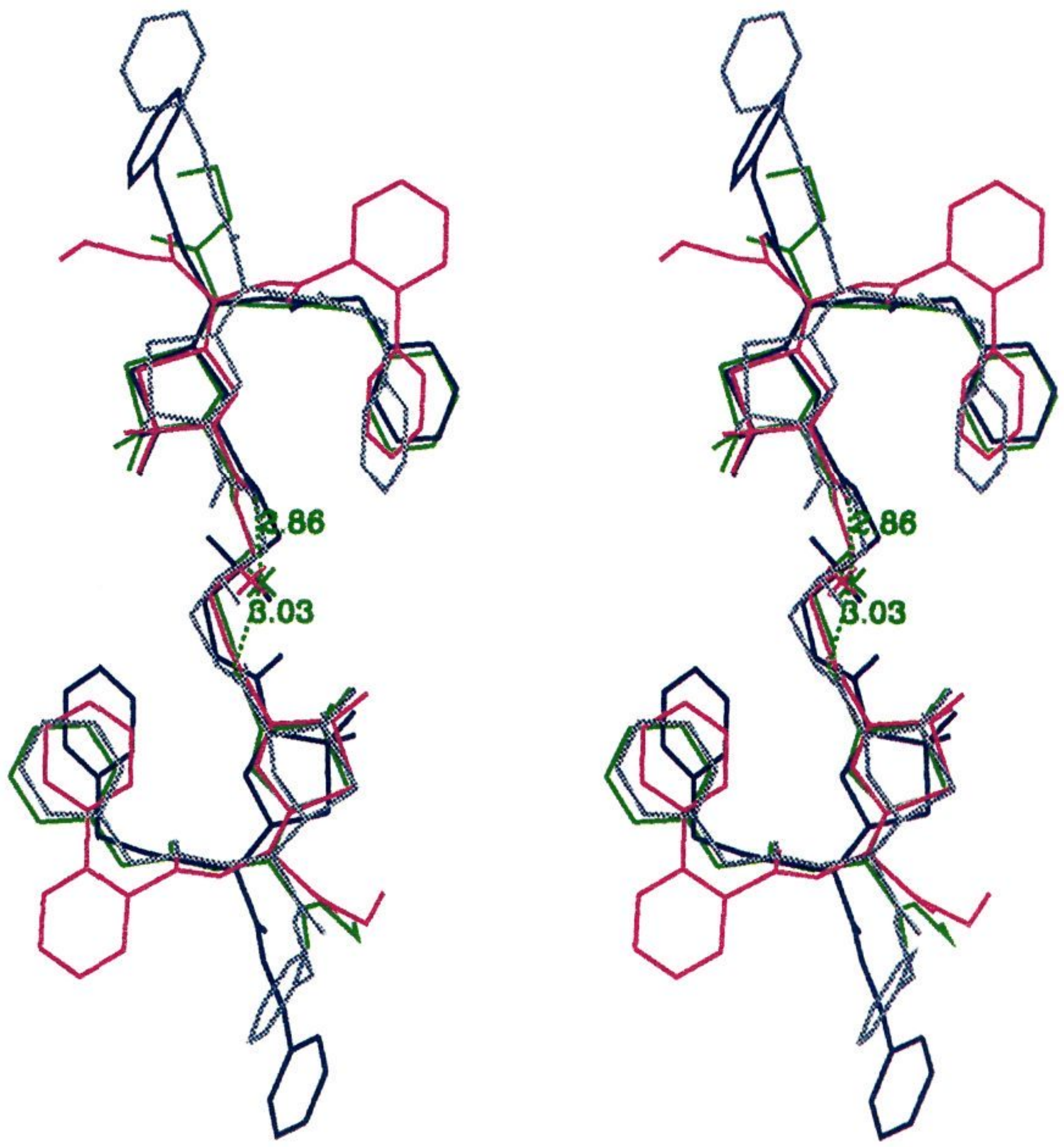

Figure 6. Overlays of ligand conformations taken from superposed HIVP complexes. Inhibitor **1** in green; **3** in red; **2** in light blue (stippled) and dark blue, representing the two alternative refined conformations of this pseudo-C_2-symmetric compound. The S_2/S_2' conformations of the three ligands are similar, although half of **2** is rotated relative to the other half, pushing the phenyl ring deeper into S_2 and rotating the linker amide. Hydrogen bonds to W301 are shown.

$P2_12_12$ and shows a root mean square deviation of 0.45 Å for one monomer Cα atoms compared to its partner. This compares with 0.33 Å for **1**, which is in the more symmetric $P6_1$ (pseudo-$P6_122$) space group. The Gly 51–NH hydrogen bond to Ile 50′ CO across the flaps is inherently asymmetric[2,6] and is in a unique orientation in complexes with **1** and **3**; the **2** complex is in the true $P6_122$ space group with the monomer in the asymmetric unit and therefore this hydrogen bond cannot be present in an ordered form.

Conclusions

The C_2-symmetric penicillin-derived dimers[5] were shown by crystallography to bind symmetrically to HIV-1 proteinase in one of the symmetric modes outlined by molecular modeling, confirming the NMR observations. These compounds trace a novel S-shaped path through the active site, with poor contacts at the catalytic aspartates, but excellent occupancy of the S_1/S_1' and S_2/S_2' subsites. The compounds are extensively hydrogen bonded and maintain the feature of water 301 that bridges between the flaps and peptide-based analogues. Good hydrophobic packing in S_1/S_1' and S_2/S_2' and maintenance of the hydrogen-bonding network are dominant forces in the binding of these compounds, and bulky groups at the edges of the active site can be deleterious to binding. The structural information enabled us to rationalize the observed SAR for the series of compounds described in this and the accompanying paper,[5] higher affinity compounds being designed from the details provided. The unique binding mode of these novel HIVP inhibitors is remarkable in that all the same protein residues are involved as are observed in the binding of more substrate-like compounds.[2,6,8,9] Further analysis of these observations may lead to improved design of inhibitors to this enzyme and to greater understanding of molecular recognition in general.

Experimental Section

Protein Purification and Crystallization. The enzyme was purified[12] and immediately inhibited with the appropriate compound. The compounds were dissolved in 250 μL dimethyl sulfoxide and added to the protein to achieve molar ratio of 10:1 with respect to the enzyme dimer. The complex was dialyzed for 3 h against 50 mm MES buffer, pH 5.0, containing 1 mM EDTA, 5 mM DTT, and 1 mM sodium azide at 4 °C. After equivalent addition of the inhibitor, the mixture was concentrated to near 4 mg/mL using Amicon YM-10 membranes (Millipore Limited). Protein crystallizations were set up using the hanging-drop vapor-diffusion method. The well solution contained 50 mM MES buffer, pH range 5.0–6.5, or 50 mM sodium acetate buffer, pH range 4.5–6.0 with 300–700 mM ammonium sulfate as precipitant. The crystals grew within a week at both 10 and 20 °C. Chemicals were from BDH, Poole, UK.

Crystal Characterization. The crystals of complexes with **1** and **2** where hexagonal crystals were obtained (Table II) showed high mosaicity and gave maximal resolution of 2.6 and 2.8 Å, respectively. For the complex with **1** the diffraction showed clear deviations from true *mm* symmetry in the *hk*0 zone, particularly at high resolution, from which the space group $P6_1$ was concluded while for **2** it was apparent the crystals behaved as if they had the higher symmetry of $P6_122$. The asymmetric unit of the crystals for the symmetric compound **1** is the complete dimer

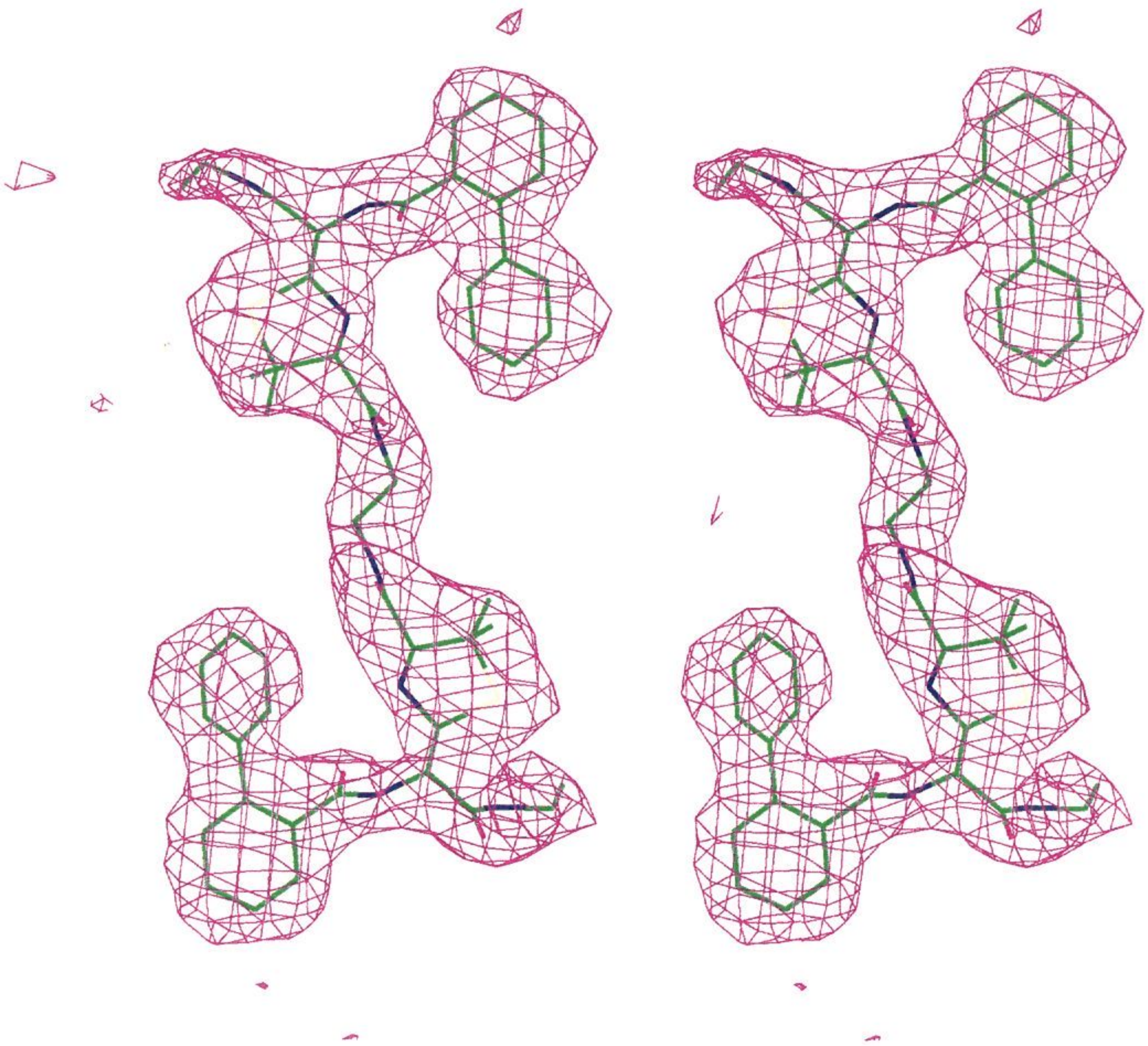

Figure 7. View of electron density of final atomic model of **3** in HIVP/**3** complex at 2.5-Å resolution. The $|F_o-F_c|\alpha_c$ electron density map was calculated from a model containing all atoms of the protein with the ligand omitted and is contoured to 2σ. The planes of the phenyl rings in S_2 are seen to be rotated by a relative angle of 60°.

whereas for compound **2** it is the monomer. For the purposes of refinement, calculations for crystals of the complex with **2** were carried out in space group $P6_1$. The orthorhombic crystals obtained in complexes with compound **3** (Table II) were of the same form as described for acetylpepstatin[9a] with the proteinase dimer as the asymmetric unit of the crystal and diffracted to at least 2.5-Å resolution.

Data Collection. All diffraction data were recorded from single crystals using a FAST area detector; for compounds **1** and **2**, use was made of beamline 9.6 at SERC Daresbury Laboratory with a wavelength of 0.89 Å while for compound **3** Cu Kα radiation from a rotating anode source was employed. In order to achieve as complete a data set as possible, two scans were collected about different axes in the crystal. The images were processed with the MADNES software package[13] and then scaled and merged with the CCP4 suite of programs.[14] The resulting merging *R* factors for symmetry-related reflections are given in Table II.

Structure Determination. The structure of the complex with **1** was solved by molecular replacement with the coordinates of the HIV protease dimer derived from the MVT-101 complex[6] using the fast rotation function (Crowther) with data from 10 to 3 Å. The correct solution was the highest peak, and was consistent with the protease dimer axis being aligned closely with the *a*-axis of the unit cell. The position of the dimer was established by a 1-D translation search calculating *R* factors at 0.6-Å intervals; this gave a clear minimum consistent with good packing in the $P6_1$ cell. Complexes with **2** and **3** were closely homologous to other known structures and required no separate solution step.

Refinement and Modeling. All structures were refined using X-PLOR[15] with initial rigid-body refinement. Water molecules were omitted from the starting models and the ligand structure modeled into electron density map using FRODO[16] after refinement of all protein atomic positions was complete. For the complex with **1** a cycle of simulated annealing at 3000 °C with a slow cooling protocol was carried out after inclusion of the ligand. Cycles of refinement were alternated with map fitting in which corrections were made to the protein model and solvent molecules added. The resulting structures have *R* factor values R_{final} given in Table II for all reflexions greater than 2σ and have typical deviations from ideal geometry of 0.02 Å for bond distances and 3.5° for bond angles.

NMR Spectroscopy. Samples for NMR experiments were inhibited and concentrated as above, with a final dialysis into 10 mM acetate-d^3 in D_2O or 90% H_2O/10% D_2O, pH 5.0. Protein concentrations ranged from 2 to 4 mg/mL. ^1H NMR spectra were recorded on a Bruker AM 500 MHz spectrometer. ^{19}F spectra were recorded on a Varian VXR 400-MHz spectrometer. All spectra were recorded at 298 K.

Molecular Modeling. The molecular models described were constructed with the aid of the INSIGHTII[17] modeling system, using, where possible, units from within the fragment library and the crystal structure of HIV proteinase/JG-365.[8a] Geometry optimization was performed using DISCOVER utilizing the CVFF force field.[18] The results were visualized using INSIGHTII running on a Silicon Graphics 4D35TG.

Acknowledgment. We thank Dr. Richard Hall and Dr. Dev Baines for the contribution to protein scale-up, Dr. Anne Cleasby for crystallographic assistance, and Dr. Alex Wlodawer (NCI, Frederick, MD) for provision of HIVP coordinates.

References

(1) Kohl, N. E.; Emini, E. A.; Schleif, W. A.; Davies, L. J.; Heimbach, J. C.; Dixon, R. A. F.; Scholnick, E. M.; Sigal, I. S. Active Human Immunodeficiency Virus Protease is Required for Viral Infectivity. *Proc. Natl. Acad. Sci. U.S.A.* **1988**, *85*, 4686–4690.

(2) (a) Erickson, J.; Neidhard, D. J.; VanDrie, Kempf, D. J.; Wang, X. C.; Norbeck, D. W. Plattner, D. J.; Rittenhouse, J. W.; Turon, M.; Wideburg, N.; Kohlbrenner, W. E.; Simmer, R.; Helfrich, R.; Paul, D. A.; Knigge, M. Design, Activity and 2.8 Å Crystal Structure of